2025
12(1), 1187

MATERIALS
NANOSCIENCE

Detection of SARS CoV biomarker Ethyl Butyrate on reduced 2-dimensional Zinc Oxide

Amretashis Sengupta

[1]*Department of Physics, P.D. Women's College, Jalpaiguri, West Bengal – 735101, India.* [2]*University of North Bengal, Dist. Darjeeling, West Bengal – 734013, India.*

Submitted on: 03-Mar-2025, Revised: 24-May-2025 Accepted: 25-May-2025, Published on: 27-May-2025

Article

ABSTRACT

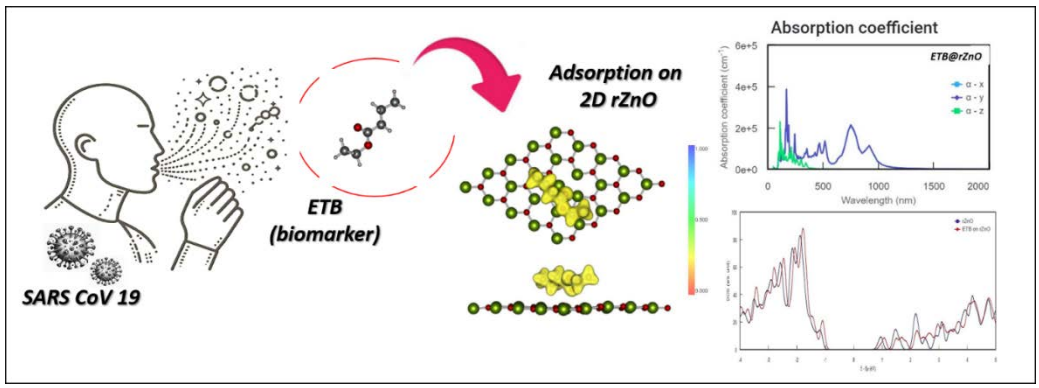

In this work we study the detection of ethyl butyrate (ETB) , a prominent SARS CoV biomarker with reduced two-dimensional (2D) ZnO. With density functional theory (DFT) calculations we show the adsorption of ETB on non-stoichiometric sites of 2D rZnO. It is seen that ETB adsorbs well on rZnO with a binding energy of around 0.8eV and shows significant changes in the electronic density of states and charge density of the 2D sheet upon ETB adsorption. The adsorbed ETB molecule tends to draw a small net positive charge of ~0.25eV/Bohr^3 around itself. The optical properties such as dielectric function and the absorption spectra undergo detectable changes in peaks even for the adsorption of a single molecule. The optical absorption spectra show emergence of a single peak at 780nm upon ETB adsorption compared to multiple peaks between 675-720nm for the bare 2D sheet. These significant changes can aid in rapid detection of the biomarker, by electronic or optical detection means, leading to the development of novel sensors for rapid SARS CoV detection.

Keywords: 2D materials, DFT, ZnO, Sensor, Biomarker

INTRODUCTION

Recently Ethyl butyrate (ETB) has been identified as a promising biomarker for identifying SARS-CoV infection due to its connection with the virus's metabolic pathways.[1] Recent studies on the volatile organic chemicals exhaled with the breath of patients infected with SARS-CoV have identified ethyl butyrate as a noteworthy molecule.[1,2] These investigations indicate that detection of ETB in breath can be a potentially rapid and non-invasive method of screening for SARS-CoV.[1,2]

Several semiconducting metal oxides such as SnO_2, ZnO, TiO_2 and many other have been hugely popular for various gas / chemical sensing applications for their exceptional sensitivity, convenient production techniques, affordability, and strong compatibility with different fabrication processes.[3–5] It is well understood that for such oxide material gas / chemical sensors the performance is significantly influenced by the surface condition, shape, and microstructure of the sensing material.[3–6] Such factors control the active area and the adsorption of different chemicals / gas molecules, thereby making a strong case for surface engineering better sensors by exploiting nanostructured materials.

Of late, 2D materials have become viable choices for chemical sensors, owing to their enhanced adsorption capabilities due to high surface-to-volume ratio, and good electrical properties enabling the detection of various molecules with great sensitivity. 2D Graphene, transition metal dichalcogenides (TMDs), black phosphorus, WO_3, AlN and 2D ZnO and its derivatives are materials that possess suitable electrical and chemical properties, which can be effectively utilized in gas sensing applications, including single molecule detection.[7–10]

2D ZnO the atomically thin counterpart of a very popular gas sensing bulk material ZnO, can be of much interest for biosensing applications.[11–14] Zinc oxide (ZnO) is considered as an excellent material for the development of gas and chemical sensors due to its non-toxic nature, affordability, and ease of synthesis. Further its bio-compatible nature[15,16] reaffirms the application of ZnO or its derivatives for biosensing devices. Therefore, in its 2D form

*Corresponding Author: Dr. Amretashis Sengupta
Email: amretashis@gmail.com

DOI:10.62110/sciencein.mns.2025.v12.1187
URN:NBN:sciencein.mns.2025.v12.1187

https://pubs.thesciencein.org/jmns

ZnO can be a very versatile material for sensing applications, which prompts us to investigate its usefulness for the detection of SARS-CoV biomarker. When it comes to the adsorption properties of ZnO, it is often observed that non-stoichiometric ZnO or reduced ZnO often shows a better surface sensitivity to chemical or gas molecules.[16] In order to achieve higher sensitivity for a biomarker that is expected in trace amounts, reduced ZnO or rZnO can be a better choice, and is worth studying.

In this work we study the detection of ETB on 2D rZnO with density functional theory calculations (DFT). We studied the adsorption properties for different orientations of the ETB molecule on both 2D ZnO and 2D rZnO sheets. We also studied the changes in the electronic and optical properties of the nanosheet upon the adsorption of ETB molecules and evaluate the prospects of 2D rZnO based rapid non-invasive SARS-CoV screening sensors.

METHODS

Our calculations involve a supercell of monolayer 2D ZnO (rZnO), as illustrated in Figure 1. The supercell has a vacuum gap of 10 Å on both sides. The DFT calculations are performed with the Quantum ESPRESSO[17] software package as implemented in Material Square. The calculations use the generalized gradient approximation (GGA) in DFT with the Perdew-Burke-Ernzerhof (PBE) exchange and correlation functional.[18] The standard solid state pseudopotentials (SSSP) PBE Efficiency v1.1.0 sets were used for the elements.[19] In the calculations, the wavefunctions were set a kinetic energy cutoff of 60 Rydberg, while the density cutoff was set at 240 Rydberg.[18,19] The supercell was discretized with a 3x3x1 Monkhorst-Pack k-point mesh.[20] The Davidson diagonalization procedure[21] was used and the electron convergence threshold was taken to be 10^{-7}Ry. The Fermi-Dirac smearing technique was considered for the electron occupations in the DFT calculations. The Grimme's DFT-D3 approach is used to introduce the van der Waals corrections in all the calculations.[22] In the structural relaxations studies the Broyden-Fletcher-Goldfarb-Shanno (BFGS) algorithm[23] was used to minimize the Hellmann-Feynman forces below 10^{-3}Ry/Bohr while the pressure convergence threshold was set at 0.005 GPa.

The adsorption energy was calculated as [12]-[16]

$$E_{ads} = E_{ETB@ZNO} - E_{ETB} - E_{ZNO} \quad \text{-- (1)}$$

Where $E_{ETB@ZNO}$, E_{ETB} and E_{ZNO} are the total energies of the ETB adsorbed 2D sheet, total energy of the isolated ETB molecule and that of the isolated 2D ZnO (rZnO) respectively.

The structural optimizations showed that ETB adsorbed favourably on 2D rZnO rather than on pure 2D ZnO, and therefore further studies such as charge density, DOS, optical properties were limited to the ETB adsorbed rZnO structure only.

The optical spectra were computed employing the random phase approximation (RPA) method, which is included in the epsilon.x toolset of ESPRESSO.[17]

RESULTS AND DISCUSSIONS

From the structural optimization calculations, different orientations of the ETB molecule and different adsorption sites were considered on 2D ZnO and 2D reduced ZnO supercell. It was observed that the adsorption of ETB molecule happened on the defect site (oxygen vacancy) of the 2D rZnO rather than on perfect ZnO. In Figure 1, we show the optimized ZnO and rZnO supercells and the optimized structure with ETB molecule adsorbed on rZnO. It is readily seen that ETB molecule adsorbed lying horizontally parallel to the surface of the 2D sheet, rather than vertically and that the oxygen atom of the ETB molecule tends to anchor generally towards the vacancy. The distance between the 2D sheet and the closest oxygen atom of ETB to the 2D surface was measured to be 2.704Å.

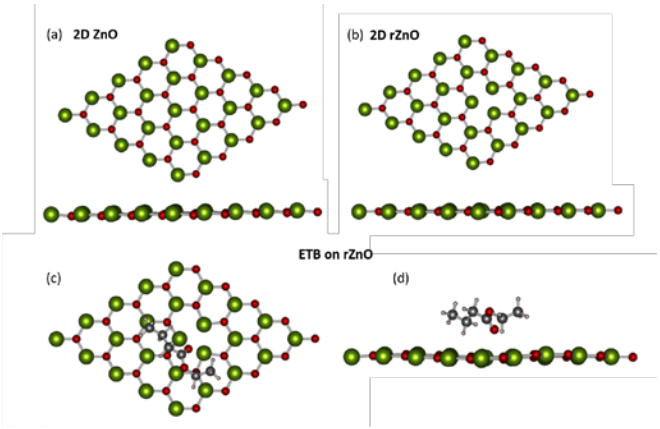

Figure 1: Supercell of (a) 2D ZnO and (b) 2D reduced ZnO (rZnO), showing views from the top (XY plane) and side (YZ plane) (c) top view of ETB molecule adsorbed on rZnO and (d) side view of ETB molecule adsorbed on rZnO.

The adsorption energy of ETB on rZnO was calculated to be 0.802eV which suggests sufficiently good binding of the biomarker to the sensing surface.

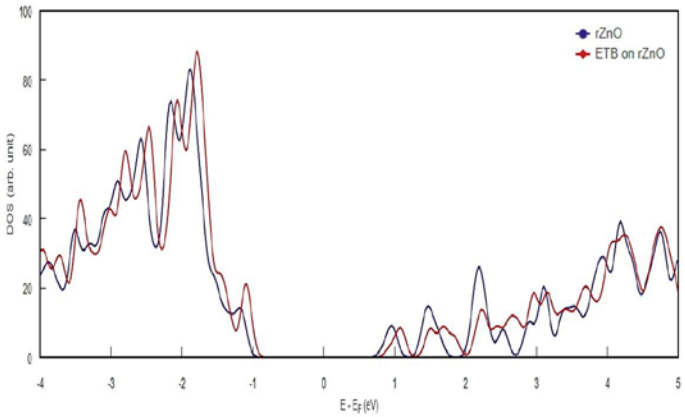

Figure 2: Density of states (DOS) of bare 2D rZnO and ETB adsorbed rZnO

In Figure 2, we show the density of states (DOS) of the 2D rZnO sheet with and without the ETB molecule adsorbed. It is quite evident from the plot that there are detectable changes in

the DOS which is a result of the changes in the electronic state of the system upon the adsorption of the biomarker. The changes are easily observable around the conduction and valence band edges, thereby making a good prospect for detection of the adsorbed single molecule of biomarker through changes in electronic transport properties of the 2D sheet. This indeed is an encouraging result for the prospect of rZnO based ETB sensors.

The results of the charge density difference (CDD) study presented in Figure 3, show an accumulation of positive charge on the ETB surface after adsorption. The adsorbed ETB molecule tends to draw a cloud of net positive charge of about 0.25e/Bohr3 around itself. Such a change in the electrostatics of the sheet is promising for easy detection of ETB molecules on 2D rZnO.

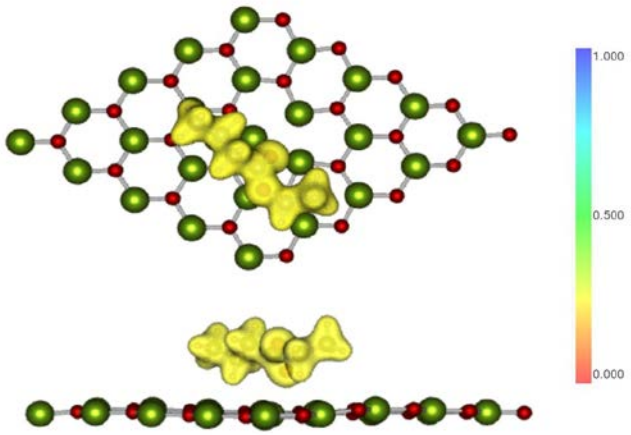

Figure 3: Charge density difference isosurface plot of ETB adsorbed rZnO.

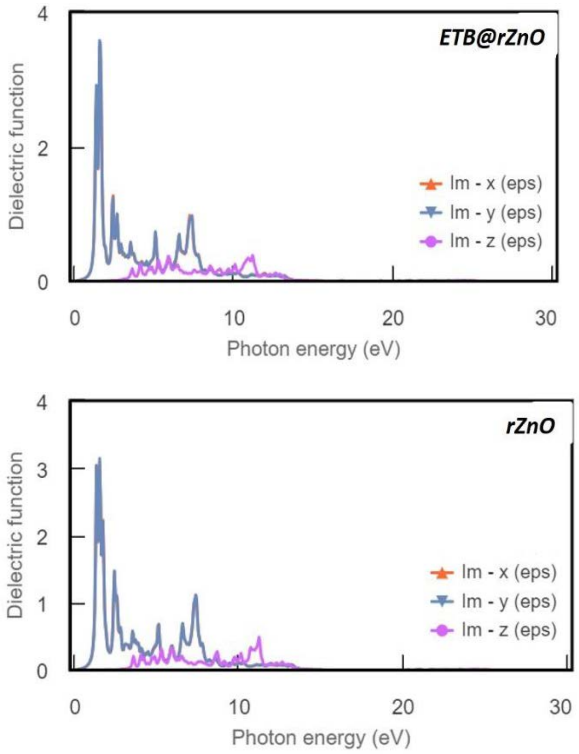

Figure 4: Imaginary part of the dielectric function of ETB adsorbed rZnO and pure rZnO.

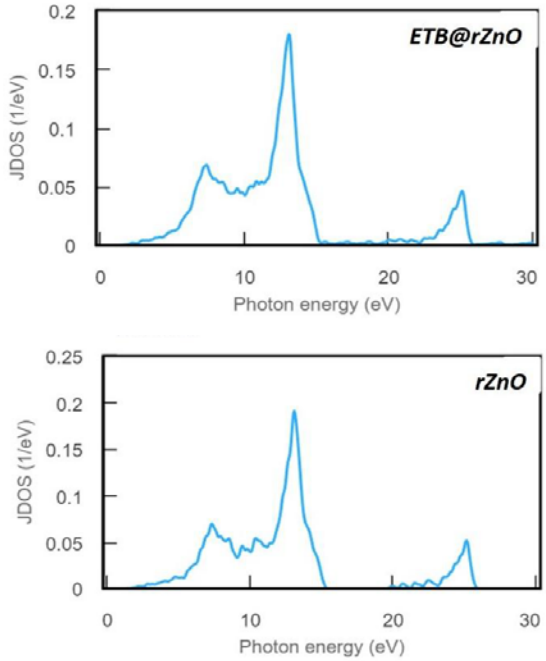

Figure 5: Joint density of states of ETB adsorbed rZnO and pure rZnO.

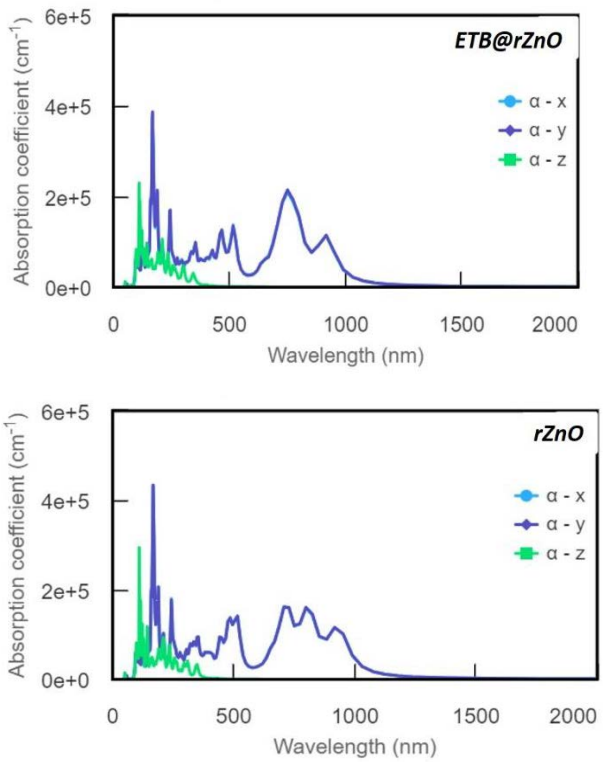

Figure 6: Absorption coefficient of ETB adsorbed rZnO and pure rZnO.

Another common method of biosensing is the measurement of optical properties of the sensing material, where there is a detectable change before and after the biomarker absorption. For this the optical properties such as dielectric function, JDOS and the optical absorption spectra were studied for both the bare rZnO

and the ETB adsorbed rZnO sheet. The optical properties of the 2D sheet, namely the imaginary dielectric function, joint density of states (JDOS) and absorption spectra (for both before and after ETB adsorption) can be seen in Figure 4, Figure 5 and Figure 6 respectively. It is observable from Figure 4 that there is a less sharp peak in the dielectric function corresponding to photon energies of 7.25eV (UV region) upon the adsorption of ETB on the 2D sheet. In the JDOS plot of Figure 5, the more prominent fluctuation in the energy range of 6.5 to 7.5eV is seen for the bare 2D sheet, as compared to the more smeared nature of JDOS in the same region for the ETB adsorbed 2D rZnO sheet. Theoretically this indicates that there is more possible optical transition between states having energy difference in the said energy range as the ETB adsorbs on 2D rZnO. This is likely the result of the charge accumulation on the ETB molecule which may alter the occupancy of certain states of the system causing a change in the optical transitions as well.

A more practical observable for experimental studies is likely to be the optical absorption, which also shows a marked change in the absorption spectra in the 600-800 nm wavelength, showing a significant shift in the absorption peak. Instead of the multiple smaller peaks around 675nm and 720nm for the bare 2D rZnO, we can see a single much stronger absorption peak appearing around 780nm. Indicating a significant observable change in the optical properties upon the biomarker adsorption of 2D rZnO, which is indeed a promising sign for ETB detection on 2D rZnO.

CONCLUSION

In this work with DFT calculations we explored the possibility of sensing ethyl butyrate (ETB) , a SARS CoV biomarker, on 2D ZnO or reduced ZnO (rZnO) sheets. The calculations show that 2D rZnO is more active in surface adsorption of ETB molecules as compared to stoichiometric ZnO. Structural optimization calculations show ETB to adsorb near to the oxygen vacancy in rZnO with the molecule lying horizontally over the 2D material. The adsorption energy of the molecule on the 2D surface was found to be 0.8eV which indicates a good binding of the biomarker. In terms of the possible avenues for detection of the adsorbed biomarker, electronic and optical property changes upon adsorption were investigated with DFT studies. It was observed that there are detectable changes in the density of states, and charge density even for a single adsorbed molecule, which suggest a good scope of electronic detection of the biomarker. Optically, marked changes in dielectric function and absorption further indicate a prospect for sensing ETB with 2D rZnO surface as the sensing element. These results hold promise for designing fast and efficient biosensors for rapid detection of a SARS-CoV-19 biomarker with 2D rZnO.

ACKNOWLEDGMENTS

The author thanks the Science and Engineering Research Board (SERB), Govt. of India for the grant no. SB/SRS/2019-20/03/ES.

CONFLICT OF INTEREST STATEMENT

Author do not have any conflict of interest for this work.

REFERENCES AND NOTES

1. H. Chen, X. Qi, L. Zhang, et al. COVID-19 screening using breath-borne volatile organic compounds. *J. Breath Res.* **2021**, 15 (4), 47104.
2. S. Xia, X. Luo. Analysis of 2D nanomaterial BC3for COVID-19 biomarker ethyl butyrate sensor. *J. Mater. Chem. B* **2021**, 9 (44), 9221–9229.
3. X. Tian, X. Cui, T. Lai, et al. Gas sensors based on TiO2 nanostructured materials for the detection of hazardous gases: A review. *Nano Mater. Sci.* **2021**, 3 (4), 390–403.
4. Y. Masuda. Recent advances in SnO2 nanostructure based gas sensors. *Sensors Actuators B Chem.* **2022**, 364, 131876.
5. M.A. Franco, P.P. Conti, R.S. Andre, D.S. Correa. A review on chemiresistive ZnO gas sensors. *Sensors and Actuators Reports* **2022**, 4, 100100.
6. H. Ji, W. Zeng, Y. Li. Gas sensing mechanisms of metal oxide semiconductors: A focus review. *Nanoscale* **2019**, 11 (47), 22664–22684.
7. S. Yang, C. Jiang, S. huai Wei. Gas sensing in 2D materials. *Appl. Phys. Rev.* **2017**, 4 (2).
8. M. Donarelli, L. Ottaviano. 2d materials for gas sensing applications: A review on graphene oxide, mos2, ws2 and phosphorene. *Sensors (Switzerland)* **2018**, 18 (11).
9. M.V. Sulleiro, A. Dominguez-Alfaro, N. Alegret, A. Silvestri, I.J. Gómez. 2D Materials towards sensing technology: From fundamentals to applications. *Sens. Bio-Sensing Res.* **2022**, 38 (July), 100540.
10. S.G. Leonardi. Two-dimensional zinc oxide nanostructures for gas sensor applications. *Chemosensors* **2017**, 5 (2).
11. H. Chen, Y. Qu, J. Ding, H. Fu. Adsorption behavior of graphene-like ZnO monolayer with oxygen vacancy defects for NO2: A DFT study. *Superlattices Microstruct.* **2019**, 134 (June), 106223.
12. R. Meng, X. Lu, S. Ingebrandt, X. Chen. Adsorption of Gas Molecules on Graphene-Like ZnO Nanosheets: The Roles of Gas Concentration, Layer Number, and Heterolayer. *Adv. Mater. Interfaces* **2017**, 4 (21), 1–10,.
13. Y. Wang, X. Yang, C. Hu, T. Wu. Rh-Doped ZnO Monolayer as a Potential Gas Sensor for Air Decomposed Species in a Ring Main Unit: A First-Principles Study. *ACS Omega* **2021**, 6 (24), 15878–15884.
14. J.H. Li, J. Wu, Y.X. Yu. DFT exploration of sensor performances of two-dimensional WO3 to ten small gases in terms of work function and band gap changes and I-V responses. *Appl. Surf. Sci.* **2021**, 546 (January), 149104.
15. S.F. Rastegar, A.A. Peyghan, H.R. Ghenaatian, N.L. Hadipour. NO 2 detection by nanosized AlN sheet in the presence of NH 3 : DFT studies. *Appl. Surf. Sci.* **2013**, 274 (2), 217–220.
16. A.K. Barui, R. Kotcherlakota, C.R. Patra. Biomedical applications of zinc oxide nanoparticles. *Inorg. Fram. as Smart Nanomedicines* **2018**, 13 (ue 10), 239–278.
17. R. Liboff. QUANTUM ESPRESSO: a modular and open-source software project for quantum simulations of materials. *J. Phys. Condens. Matter* **2002**, 21, 395502.
18. J.P. Perdew, K. Burke, M. Ernzerhof. Generalized gradient approximation made simple. *Phys. Rev. Lett.* **1996**, 77 (18), 3865–3868.
19. G. Prandini, A. Marrazzo, I.E. Castelli, N. Mounet, N. Marzari. Precision and efficiency in solid-state pseudopotential calculations. *npj Comput. Mater.* **2018**, 4 (1), 72.
20. D. Vanderbilt. Soft self-consistent pseudopotentials in a generalized eigenvalue formalism. *Phys. Rev. B* **1990**, 41 (11), 7892–7895.
21. D. DeTar. Methods in computational molecular physics. *Comput. Chem.* **1985**, 9 (1), 78.
22. S. Grimme, J. Antony, S. Ehrlich, H. Krieg. A consistent and accurate ab initio parametrization of density functional dispersion correction (DFT-D) for the 94 elements H-Pu. *J. Chem. Phys.* **2010**, 132 (15).
23. J.D. Head, M.C. Zerner. A Broyden-Fletcher-Goldfarb-Shanno optimization procedure for molecular geometries. *Chem. Phys. Lett.* **1985**, 122 (3), 264–270.